**Ti-XANES ANALYSES OF SPINEL IN COARSE-GRAINED REFRACTORY INCLUSIONS FROM ALLENDE.** S. B. Simon[1], S. R. Sutton[1] and L. Grossman[1,2], [1]Dept. of the Geophysical Sci., 5734 S. Ellis Ave., Univ. of Chicago, Chicago, IL 60637 (sbs8@uchicago.edu) [2]The Enrico Fermi Institute, 5640 S. Ellis Ave., Univ. of Chicago, Chicago, IL 60637.

**Introduction:** Refractory inclusions, or CAIs, can serve as recorders of conditions in the early solar nebula. One feature of their formation environment that we can learn about from CAIs is oxygen fugacity. A system of solar composition is so reducing that it can stabilize $Ti^{3+}$, making its presence a valuable indicator of equilibration at solar $f_{O2}$ conditions. The $Ti^{3+}/Ti^{4+}$ ratios observed in the Ti-rich phases fassaite and rhönite in coarse-grained refractory inclusions have been quantitatively shown [1,2] to be consistent with formation in a gas of solar composition, one of the few features of chondrites for which this is the case.

Spinel in Murchison inclusions has a range of $Ti^{3+}/(Ti^{3+} + Ti^{4+})$ ratios of 0.2 – 0.7 [3]. Since we know the $f_{O2}$ of formation of fassaite-bearing inclusions, determination of $Ti^{3+}/Ti^{4+}$ ratios of spinel in them could allow us to relate that parameter to $f_{O2}$, allowing use of the valence of Ti in spinel as an oxybarometer. Although it has much lower Ti contents than fassaite, the valence of Ti in spinel is measurable by X-ray absorption near edge structure (XANES) spectroscopy.

In the present work we apply XANES to spinel in each of the major types of coarse-grained refractory inclusions found in Allende (CV3): compact Type A (TS19, described by [4]); fluffy Type A (TS24 [5]); Type B1 (TS34 [6]); and Type B2 (TS21 [7]). We analyzed spinel enclosed in fassaite cores and rims, in melilite, and at grain boundaries to see if the valence of Ti in spinel varies with petrographic setting.

**Analytical methods:** Samples were documented by electron microscope and analyzed by electron probe (EMP). Titanium K XANES spectra were collected at the Advanced Photon Source, using the GSECARS X-ray microprobe in fluorescence mode, with a 3 µm X-ray beam. Valences were determined following the results of [8]. That study demonstrated that Ti K-edge XANES spectra of pure $Ti^{4+}$-bearing minerals fall into two, distinct valence-coordination clusters on a plot of pre-edge peak intensity *vs.* energy. Those with all Ti in tetrahedral coordination have high intensities and low energies, whereas those with all Ti in octahedral coordination have low intensities and high energies. Any $Ti^{3+}$ present in spinel is expected to be in octahedral coordination, yielding a third data cluster, pre-edge peaks with relatively low intensity and low energy [9]. Titanium valences in unknowns were determined by applying the lever rule to mixing lines for XANES results for standards representing these three endmember occurrences. Valences are reported as values between 3 and 4. Low valences, ~3, reflect high $Ti^{3+}/Ti^{4+}$. Most analyses have uncertainties of ±0.06.

**Sample Details:** The spinel analyzed in the CTA is coarse (100-200 µm across), subhedral to euhedral, and enclosed in melilite or melilite and perovskite. It is nearly pure $MgAl_2O_4$ with <0.5 wt% FeO, ~1 wt% $V_2O_3$, ~0.5 wt% $TiO_2$ and ~0.5 wt% $Cr_2O_3$. Spinel in the FTA, not analyzed by EMP, is finer and enclosed in melilite. That in the Type B inclusions is coarse, euhedral, and enclosed in either fassaite or melilite or is at a boundary between phases. Analyzed spinel in the Type Bs contains 0.3-0.7 wt% $TiO_2$ and 0.2-0.4 wt% $V_2O_3$ and $Cr_2O_3$.

**Results:** Valences are listed in Table 1 and illustrated in Fig. 1. The spinel grains in TS19 (CTA) that are in contact with perovskite have Ti valences within error of 4.0 (3.98±0.06; 3.96±0.06). Other grains have valences between 3.8 and 3.9. The valence in the core of one grain is 3.91 and that of its rim is 3.82. Spinels in TS24 (FTA) have valences from 3.74 to 3.90. The analyses of TS19 spinel average 3.90±0.03 and the TS24 analyses average 3.80±0.03.

Ti valence in spinel in the Type B inclusions exhibits a wider range than that in the Type As. In TS34, values range from 3.57 to 4.02±0.06. Spinel in fassaite has higher Ti valence than its host. The grains with the lowest valences, 3.57 and 3.68, occur in the Ti-rich interior of a coarse, zoned fassaite with Ti valences (by EMP) of 3.20 and 3.13, respectively. Toward the edge of this fassaite grain, the Ti in the spinel is more oxidized (3.88) and so is the fassaite (3.24). The TS34 spinel with the highest Ti valence is in contact with Ti-poor fassaite, late melilite ($Åk_{\sim70}$) and secondary alteration products. The Ti contents of the spinels mimic those of their hosts, resulting in an inverse correlation between Ti valence and Ti content in TS34 spinels (Fig. 1).

The range of Ti valences in spinel in TS21 (Table 1) is 3.52-3.83, similar to that in TS34, despite a narrower range of $TiO_2$ contents (Fig. 1). A traverse across Sp7 (Fig. 2) shows a range of 3.60-3.83, with a valence increase followed by a sharp decrease ~8µm from the center. This grain, enclosed in melilite ($Åk_{45}$), and one (Sp6) enclosed in anorthite and monticellite are more oxidized than grains (Sp4, 5) that are enclosed in fassaite.

**Discussion:** While spinel does not show a preference for either $Ti^{3+}$ or $Ti^{4+}$ relative to coexisting hibonite or Al-diopside in Murchison inclusions [3], we do know that fassaite favors $Ti^{3+}$ over $Ti^{4+}$ [6]. This may explain why spinel in the Type B inclusions has lower $Ti^{3+}$ proportions than enclosing fassaite, and spinel in the Type As, with Ti valences of 3.8-3.9, has higher valences than most CTA fassaite (3.2-3.4).

There is a relationship between petrographic setting and valence of Ti in spinel. In TS19, spinel in contact with perovskite has nearly pure $Ti^{4+}$, possibly due to local $Ti^{4+}$ enrichment from perovskite dissolution [10] and incorporation into spinel before reduction could occur. In both Type B inclusions studied, spinel in contact with alteration products has higher proportions of $Ti^{4+}$ than grains completely enclosed in fassaite. The low $Ti^{3+}$ proportions in spinel that is in contact with secondary alteration products suggest that the valence of Ti in spinel was affected by late-stage events.

In Type B1 inclusions, fassaite is zoned with decreasing $Ti^{tot}$ and $Ti^{3+}/Ti^{4+}$ from core to rims of grains [6]. The spinel in TS34 mimics this trend (Fig. 1), reflecting the changing liquid composition during fractional crystallization. Thus spinel enclosed in early, $Ti^{tot}$-, $Ti^{3+}$-rich fassaite is itself richer in $Ti^{tot}$ and $Ti^{3+}$ than spinel enclosed in later-formed fassaite. Some spinels in TS34 are zoned from low-$Ti^{3+}/Ti^{4+}$ cores to high-$Ti^{3+}/Ti^{4+}$ rims [11]. These grains may have relict cores that inherited $Ti^{4+}$ during perovskite dissolution, as described above.

The TS34 trend (Fig. 1) is not seen in the TS21 (Type B2) data. Because this inclusion lacks a melilite mantle to seal off the interior from the nebular gas, its late liquid did not become $Ti^{3+}$-poor [7].

**Table 1.** Valence of Ti in spinel in Allende CAIs.

| **TS19 (CTA)** | Ti valence | 1σ unc. |
|---|---|---|
| Spinel 8 | **3.98** | 0.06 |
| Spinel 9a | **3.96** | 0.06 |
| Spinel 10 | **3.82** | 0.06 |
| Spinel 3c | **3.91** | 0.06 |
| Spinel 3r1 | **3.82** | 0.06 |
| Spinel Mean | **3.90** | 0.03 |
| **TS24 (FTA)** | | |
| Spinel 1 | **3.90** | 0.06 |
| Spinel 2 | **3.77** | 0.06 |
| Spinel 3 | **3.79** | 0.05 |
| Spinel 4 | **3.74** | 0.06 |
| Spinel Mean | **3.80** | 0.03 |
| **TS34 (B1)** | | |
| Spinel 1 | **3.88** | 0.06 |
| Spinel 2 | **3.68** | 0.06 |
| Spinel 3 | **3.57** | 0.06 |
| Spinel 4 | **3.84** | 0.07 |
| Spinel 5 | **3.82** | 0.06 |
| Spinel 6 | **4.02** | 0.06 |
| Spinel 7 | **3.75** | 0.06 |
| Spinel Mean | **3.79** | 0.02 |
| **TS21 (B2)** | | |
| Spinel 4 | **3.60** | 0.06 |
| Spinel 5 | **3.52** | 0.06 |
| Spinel 6 | **3.77** | 0.06 |
| Spinel 7 Mean | **3.74** | 0.02 |

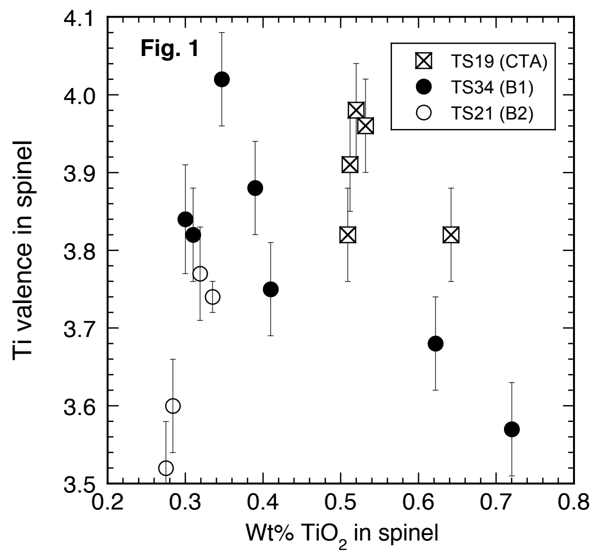


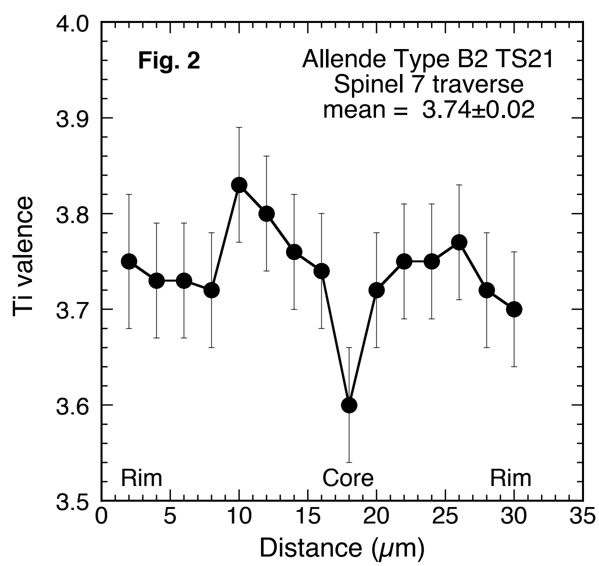


**References:** [1] Grossman L. et al. (2008) *RiMG, 68,* 93–140. [2] Beckett J. R. et al. (1986) *Meteoritics, 21,* 332-333. [3] Simon S. B. et al. (2009) *LPS XL,* Abstract #1626. [4] Simon S. B. et al. (1999) *GCA, 63,* 1233-1248. [5] MacPherson G. J. and Grossman L. (1984) *GCA, 48,* 29-46. [6] Simon S. B. et al. (1991) *GCA, 55,* 2635-3655. [7] Simon S. B. and Grossman L. (2006) *GCA, 70,* 780-798. [8] Farges F. et al. (1997) *Phys. Rev. B, 56,* 1809-1819. [9] Simon S. B. et al. (2007) *LPS XXXVIII,* Abstract #1892. [10] Paque J. M. et al. (2009) *MAPS, 44*, 665-287. [11] Paque J. M. et al. (2010) This vol.